

Progress in Smart Rotor Research for Wind Turbines: Experimental and Computational Approaches to Active Aerodynamic Control

A.K. Barlas, Wind Energy Research Group, Delft University of Technology, Kluyverweg
1, Delft, The Netherlands.

Abstract

Active distributed aerodynamic control for load reduction on wind turbine blades is an innovative concept, inspired by rotorcraft research, often named as smart rotor control. In this stage of research, unsteady aerodynamic models and small scale experimental setups are developed, investigating the potential and implementation of such concepts. This paper describes a successful wind tunnel experiment on a dynamically scaled wind turbine blade with feedback controlled deformable trailing edge geometry, based on smart material actuation, for load reduction. Also, computational efforts on smart rotor modelling concerning unsteady section aerodynamics for flapped airfoils, and ongoing work on unsteady wake models are presented. Results for representative test cases are shown. Research work is performed at Delft University Wind Energy Research Institute (DUWIND), partially funded by EU's project "UPWIND".

Nomenclature

Cl: lift coefficient
Cm: pitching moment coefficient
Ch: flap hinge moment coefficient
b: airfoil semi-chord [m]
V: wind speed [m/s]
h: plunge amplitude [m]
 α : angle of attack [rad]
a: dimensionless pitch axis location
F: geometric constants for flap
 α_{qs} : quasi-steady angle of attack [rad]
 δ_{qs} : quasi-steady angle of attack due to flap deflection [rad]
wg: vertical gust field velocity [m/s]
z: aerodynamic lag states

Introduction - Motivation

Reducing loads on wind turbine rotors can offer great reduction to the total cost of wind turbines. With the increasing size of wind turbine blades, the need for more sophisticated load control techniques has induced the interest for locally distributed aerodynamic control systems with build-in intelligence on the blades (often named in popular terms "smart structures" or "smart rotor control"). Recent inventory of design options for such systems has been performed by Barlas [1] [2]. Active load control through trailing edge flaps or deformable trailing edge geometry is considered a feasible and efficient solution, especially because of the advances in smart material actuator technology. Previous work of various research groups with CFD [3], 2D aeroelastic models [4],[5], [6] and extended BEM models [7] simulations, has shown the potential of applying active control through variable geometry

trailing edge airfoils on wind turbine blades for load reduction purposes. Also, wind tunnel tests [8] have quantified unsteady aerodynamic phenomena associated with prescribed excitation and control actions for certain 2D configurations. Consequently, the necessity for small scale experimental setups proving the active load control concept, taking the interaction of aerodynamics and dynamics of the structure into account and measuring the real performance in reduction of structural loads rises. Also, essential is the development of efficient computational models, which provide realistic evaluation of active load reduction concepts, give insight into unsteady aerodynamic and aeroelastic phenomena and serve as preliminary design platforms for wind turbine smart rotors especially concerning the controller design.

Feedback control experiments

Three wind tunnel experiments of wind turbine blades have been scheduled at DUWIND. A completed non-rotating test of a smart blade, which will be described thoroughly here, a 2D test of the aerodynamics of a (controllable) blade section in unsteady motion and a full rotating case of a wind turbine equipped with smart blades (tested in the Open Jet Facility wind tunnel at TU Delft).

In DUWIND the non-rotating wind tunnel experimental setup was prepared. The prototype of a scaled wind turbine blade was designed with embedded load reduction control devices and feedback control was applied during experiments at the TU Delft Low Speed Low Turbulence Wind Tunnel. The design of the setup from the structural point of view is shown in [9]. The ultimate goal of the approach was to show that vibrations in scaled down blade due to unexpectedly varying aerodynamic loads can be significantly reduced using trailing edge devices with an active control system. The 90cm long blade model with a 12 cm constant chord, constant thickness and no twist along the span was attached to the (specially designed) pitch system at the wind tunnel roof and it was free to deflect over a table at the free end (Fig. 1). The table ensured that no tip effects would occur that add uncertainties to measurement data. The pitch system could change the angle of attack at the blade with high speed and precision. The glass-epoxy composite blade was designed to be representative of the dynamics of a large scale wind turbine blade. The scaling parameter used was the reduced frequency k . It was used to scale the wind field disturbance (multiples of angular frequency - 1P and 3P were considered important) as well as the first flapping natural frequency on the blade (since the devices will try to reduce the vibrations in the flapwise direction). The first flapping natural frequency was tailored during the structural design of the blade (by tuning the stiffness). The aerodynamic excitation was simulated by the pitch excitation system. The scaled 1P, 3P and first flapping natural frequency of the blade were 3.5, 10.5 and 12.5 Hz respectively. The aerodynamic control devices used were based on the concept of deformable trailing edge (or partly camber control). Four Thunder[®] TH-6R piezoelectric bender actuators were used, forming two different flaps of 50% chord length size placed near the tip. The thin actuators were covered with soft foam, in order to keep the trailing edge aerodynamic shape, and a latex skin, which can expand under the actuator deflection, providing a smooth aerodynamic surface (Fig. 2). A piezoceramic patch (PZT) was used in the blade root in order to measure the change in flapping bending strains and an accelerometer at the blade tip to measure the change in acceleration of the deflecting tip. Because the interest was in the vibration reduction control, no direct aerodynamic measurements were carried out, so detailed aerodynamic phenomena cannot be quantified. Control was applied using a dSpace[®] system linked to the Control Desk GUI in Matlab Simulink[®].



Fig 1: *The adaptive blade at the LSLT wind tunnel test section*

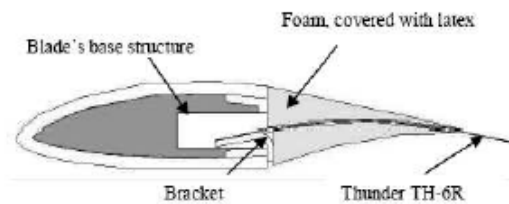


Fig 2: *Design and mounting of the actuators*

The main tests that have been carried out concern feed forward (open loop) and feedback (closed loop) control cases. For the feed forward cases, sinusoidal motions of the pitch and the counter-acting (both) flaps for different amplitudes and frequencies were carried out. Furthermore, measurements at different mean angles of attack of interest were performed, also at stall conditions. The sensitivity of the phase angle between the two motions was examined. In this way the maximum reduction in the fluctuating loads for prescribed (known) motions of excitation and actuation was shown. The maximum reduction ranges were up to 90%, especially near the natural frequency of the blade, where vibrations are amplified. A representative result is shown in Fig. 3.

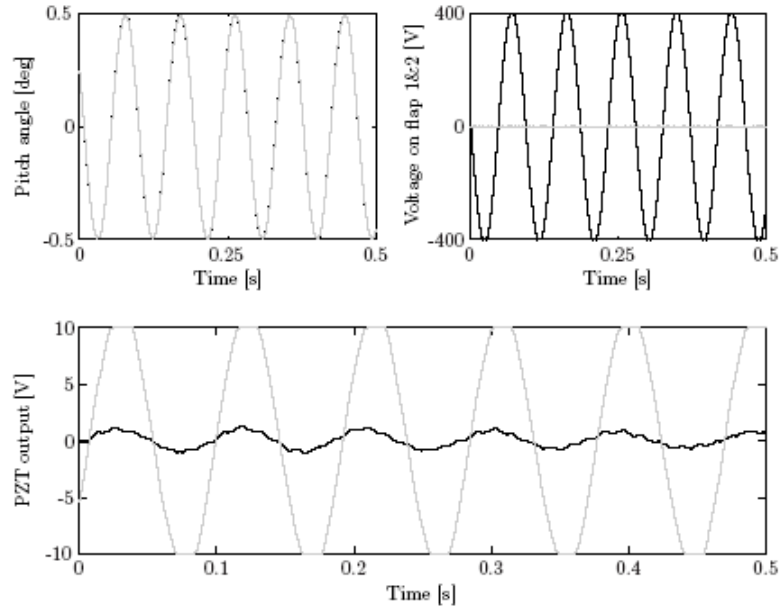


Fig 3: Reduction in root strain fluctuations for the case of a sinusoidal pitch excitation of 12.5 Hz with 0.5 degrees amplitude around angle of attack of 5 degrees at 45 m/s with prescribed counter-acting flaps motion (feed forward control) ($1V=21.3\mu$ strain). Grey line: without flaps, Black line: feed forward control of flaps.

For the feedback control tests, the transfer function of the dynamics of the system was constructed using the subspace system identification method, based on step and noise signals for the pitch actuator and the (both) flaps respectively. From that, a loop-shaped controller was designed, tuned and applied in dSpace. The input excitation cases were a sinusoidal, a step and a random signal, for different amplitudes and frequencies of interest, simulating various aerodynamic excitations like gusts and turbulence. The controller performance was great, reducing the fluctuations in root bending stresses for all cases (maximum reduction of root strains 90% for a sinusoidal disturbance, significant damping of the first eigenfrequency of the blade with a step disturbance). Representative results are shown in Fig. 4 for the step input case. For the random signal (representative noise signal) mimicking turbulence with 1P and 2P excitations, although the signal is completely unknown for the controller, it showed very good performance, leading to reductions in the load spectrum, of 37% in the scaled 1P frequency and 60% in the scaled 3P frequency.

The experimental investigations will continue with the case of a small scale rotor, incorporating spanwise active control devices, where by application of real-time feedback control the reduction in blade loads for a realistic rotating operation will be shown.

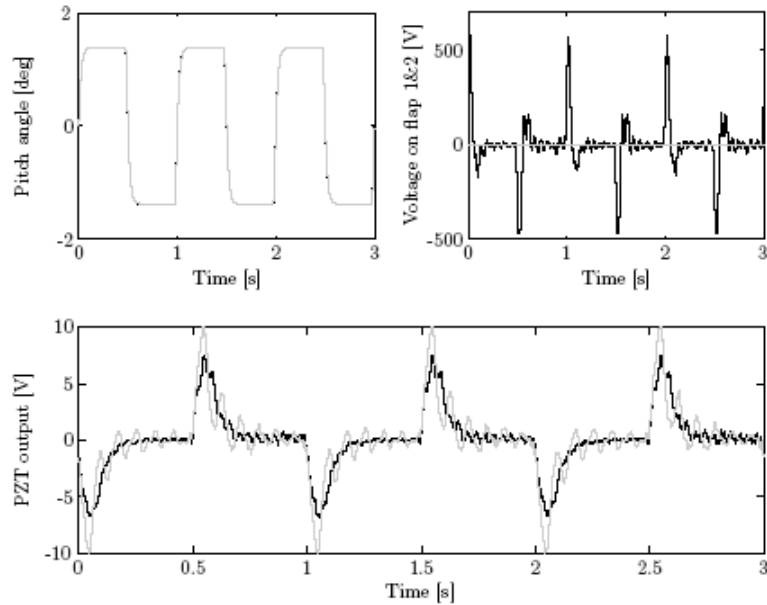


Fig. 4: Reduction in root strain fluctuations for the case of a step pitch disturbance at angle of attack of 5 degrees at 45 m/s with feedback controlled flaps motion ($1V=21.3\mu$ strain). Grey line: without flaps, Black line: feedback control of flaps.

Unsteady aerodynamics models

For the evaluation of the load reduction potential of active control devices on wind turbine blades, efficient 2d and 3d models are needed. The 2d airfoil unsteady aerodynamic behavior, but also the global 3d unsteady behaviors of such “smart” rotors are important for correct predictions. Also, aeroelastic effects should be added, since the main concern is the reduction of fatigue loads on blades. A computational model of unsteady aerodynamics for airfoils with trailing edge flaps undergoing arbitrary forcing motions will be presented here. Certain test cases will be shown, illustrating the most important aspects. Also, ongoing modeling on unsteady wake behavior of rotors with irregular time-varying blade loads will be analyzed. Effort has been put also on rotor aeroelastic modeling incorporating the above models, but will not be presented here.

At certain operating conditions, and especially when incorporating fast aerodynamic control devices, the aerodynamic response of an airfoil to various inputs (airfoil and control devices motions, wind input) is far from quasi-steady. For the prediction of unsteady aerodynamic forces, non-trivial time-domain solutions, with application to aeroelastic analysis, need to be developed. Solutions for harmonic forcing inputs in the frequency domain are of course available (see Theodorsen [10] or Bisplinghoff [11]), but in the time domain, for various arbitrary forcing inputs, the parameter of reduced frequency ($k=\omega c/2V$) in the models, becomes ambiguous. For helicopter applications, derivations of such models have been presented (see Leishman [12], [13]).

A model based on this work from helicopters has been developed. The modeling is based on thin airfoil theory for a flat airfoil with a flat (rigid) TE flap. The unsteady lift coefficient (C_l), pitching moment coefficient (C_m) and flap hinge moment coefficient (C_h) can be calculated. The calculations are only valid for small perturbations in the linear region of the C_l -alpha curve. The model is using the indicial theory concept by superimposing the effect of various arbitrary forcing inputs based on their indicial (step) response on the aerodynamic forces and moments (convolution). It is formulated in state-space form for efficient time integration and controller design. The available arbitrary forcing inputs are: airfoil pitch and plunge motions, TE flap deflection and vertical gust field. The procedure for the calculation of the unsteady C_l is shown here. The same idea holds for the C_m and C_h . The unsteady C_l is comprised of the

non-circulatory part (due to the acceleration of the airfoil in the fluid, [Eq. 2]), which can be calculated directly by the instantaneous values and rates of the motions, and the circulatory part (due to the influence of the shed vorticity, [Eq. 3]), which causes both an amplitude change and a phase delay (lead or lag). The circulatory part is calculated by superimposing the effect of all the forcing inputs. These effects are estimated by the use of Duhamel superposition integral, so calculating the response to an arbitrary input when the response to an indicial (step) input is known. The indicial responses for thin airfoils are known from theory. For the airfoil or trailing edge flap motion the response is given by the Wagner function. This is the same for airfoil motion or trailing edge flap deflection, since the circulatory lift lag is an intrinsic function of the fluid and does not depend on the airfoil boundary conditions [12]. On the other hand the Küssner function is used for the indicial response to a sharp vertical gust field. For practical reasons, both functions can be replaced by exponential approximations. Once the indicial responses are known, the impulsive responses can be calculated. The transfer function of the lag system can be calculated by taking the Laplace transform of the impulsive responses. This transfer function can be easily put in controllable canonical (state-space) form ([Eq. 4] and [Eq. 5]). The parameters in the A, B, C, D matrices are evaluated from the exponential approximations of the Wagner and Küssner functions. All effects of forcing functions can be combined in one state-space system (with the aerodynamic lag states being z , as many as the forcing functions), making the evaluation of the circulatory part of the Cl computationally efficient. State-space form is also practical for implementation into aeroelastic models and especially for control design. The full aerodynamic system can be represented by 4 states (2 for arbitrary airfoil and flap motion and 2 for the gust field). The unsteady Cm and Ch can be calculated similarly, with equivalent formulations for the non-circulatory and circulatory parts.

$$C_L = C_L^{nc} + C_L^c \quad (\text{Eq. 1})$$

$$C_L^{nc} = \frac{\pi b}{V^2} (\dot{h} + V\dot{\alpha} - ba\ddot{\alpha}) + \frac{b}{V^2} (-VF_4\dot{\delta} - bF_1\ddot{\delta}) \quad (\text{Eq. 2})$$

$$C_L^c = (C_L^c)_\alpha + (C_L^c)_\delta + (C_L^c)_{wg} \quad (\text{Eq. 3})$$

$$\begin{Bmatrix} \dot{z}_1 \\ \dot{z}_2 \\ \dot{z}_3 \\ \dot{z}_4 \end{Bmatrix} = [A] \begin{Bmatrix} z_1 \\ z_2 \\ z_3 \\ z_4 \end{Bmatrix} + [B] \begin{Bmatrix} \alpha_{qs} + \delta_{qs} \\ \frac{wg}{V} \end{Bmatrix} \quad (\text{Eq. 4})$$

$$(C_L^c)_{\alpha,\delta,wg} = [C] \begin{Bmatrix} z_1 \\ z_2 \\ z_3 \\ z_4 \end{Bmatrix} + [D](\alpha_{qs} + \delta_{qs}) \quad (\text{Eq. 5})$$

Various test cases are investigated. The first ones refer to the operating conditions of the feed-forward (prescribed) cases of the experiment, which was described above. The response of the

aerodynamic system to harmonic and step excitations for flap motion and vertical gust field is shown (Fig. 5, 6, 7).

Response of C_l to a harmonic input in flap angle (+5 deg. around aoa 8.62 deg. at 3.5Hz, $V=45\text{m/s}$)

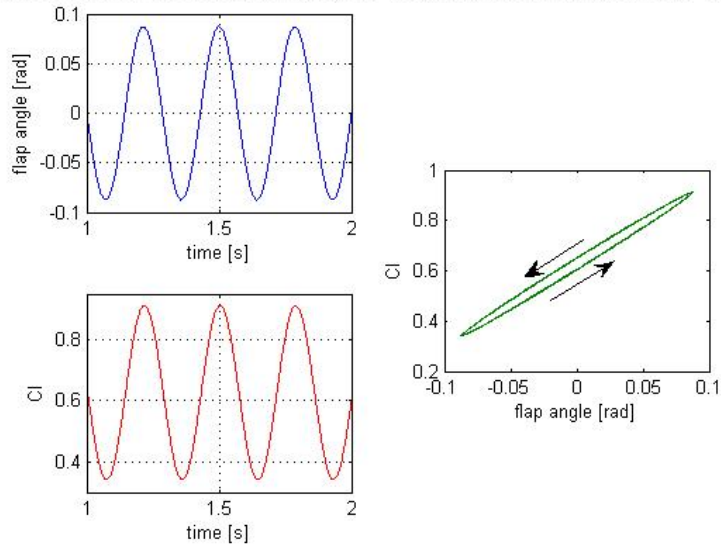


Fig. 5: Response of C_l to harmonic flap deflection.

Response of C_l to step input in flap angle (5 deg. at aoa 8.62 deg.) at 45 m/s

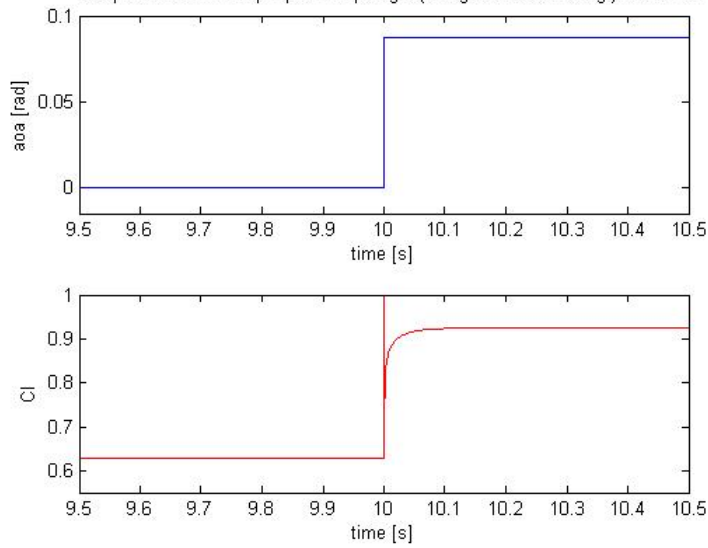


Fig. 6: Response of C_l to a step in flap deflection

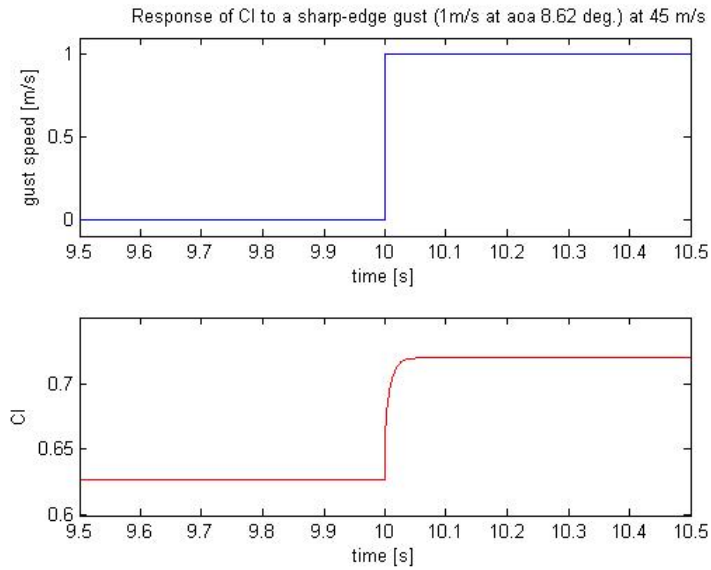


Fig. 7: *Response of C_l to a sharp-edge vertical gust.*

From the above results, we can see the effect of the unsteady aerodynamic response, with a clear time lag (although small in these specific reduced frequencies of the experiment). The effect of the transient response due to the unsteady aerodynamic functions can be seen in the cases with indicial (step) inputs.

For different operating conditions, referring to a rotating airfoil section (located near the blade tip) with a 10% trailing edge flap in a 5MW reference wind turbine blade, some cases have been investigated, including feedback control for the flap motion. The case presented here is the unsteady aerodynamic response to a turbulent wind field (with 10% turbulence intensity) for the baseline airfoil and for the airfoil including a 10% trailing edge flap, which by the use of a simple PI controller based on the measured C_l reduces the variations around the design C_l . We see that with a simple control strategy the fluctuations of C_l , as well as of C_m and C_h , are considerably reduced (98%) with flap deflections in the order of 6 degrees.

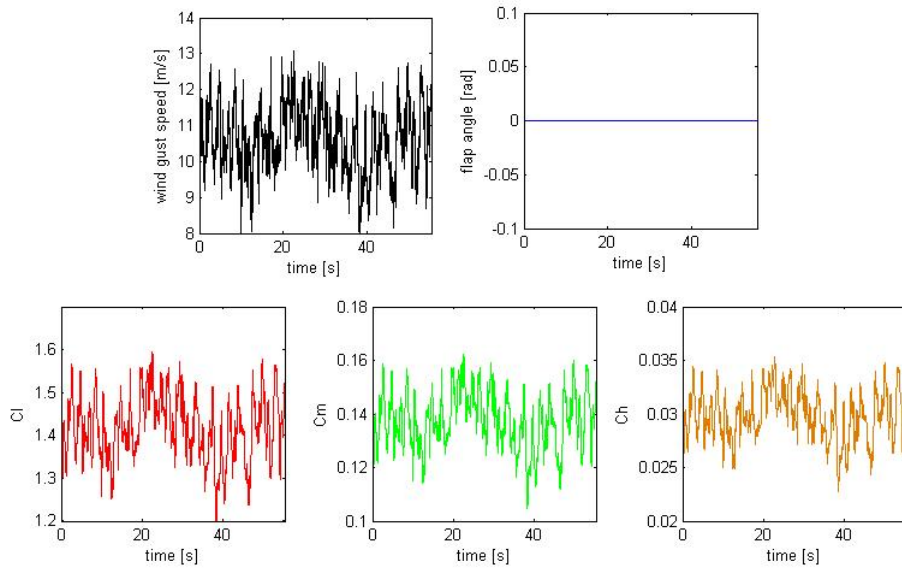


Fig. 8: Inputs and response of system for a turbulent wind speed input – No control of TE flap

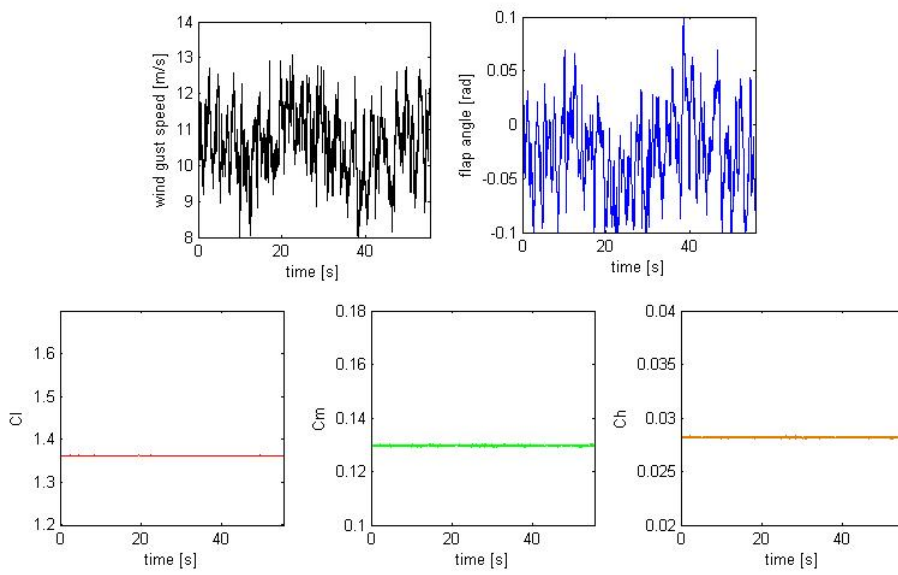


Fig. 9: Inputs and response of system for a turbulent wind speed input – Feedback control of TE flap

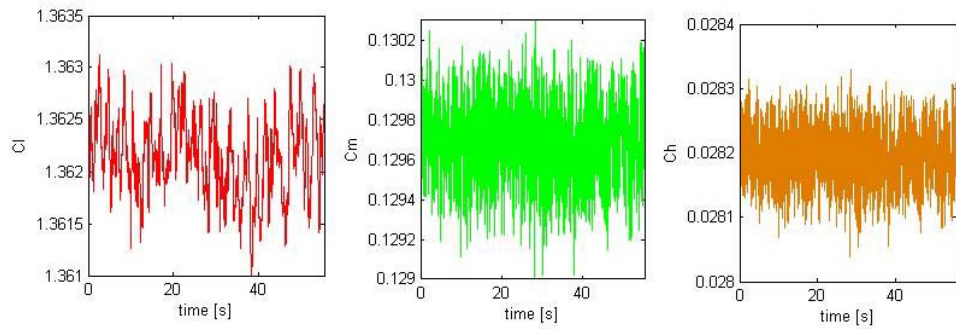


Fig. 10: Response of system for a turbulent wind speed input – Feedback control of TE flap (zoom in)

Ongoing research is also taking place regarding the 3d rotor unsteady behavior, and more specifically the dynamic behavior of the helical wake of a “smart” rotor and its effect on the induction on the rotor plane. The use of aerodynamic control devices on spanwise locations on a rotor blade causes highly unsteady loading on the blades. Because of this spatial and temporal changes in bound circulation, the distribution of vorticity in the wake changes, consequently affecting the induced velocities on the rotor plane. Previous work has shown the importance of the higher harmonic varying induction due to yaw misalignment [14]. In order to simulate the effect of the control devices on a “smart” rotor, a model has been developed, based on work of Sant [14]. This model consists of a prescribed vortex-lattice lifting line method, where time-varying bound circulation of any span-wise location can be inputted. The (fixed) wake geometry is modeled based on semi-empirical rules. In Fig. 11 and 12, for the case of a yaw misalignment of 30 degrees, the wake geometry and the induced velocities on the rotor plane are shown. The bound circulation as well as the parameters for the fixed wake was taken from experimental measurements of Sant [14]. The same approach will be taken for the case of controllable aerodynamic devices near the blade tip. The unsteady bound circulation will be calculated using the Kutta-Joukowski theorem for every spanwise location. For the sections with control actions, the previously presented unsteady aerodynamic model will be used to calculate the unsteady C_l . Because the resultant velocity in the Kutta-Joukowski theorem includes the induced velocities, an iteration loop will be used to converge to the final values for the induction on the rotor plane. Research in this field is still in progress.

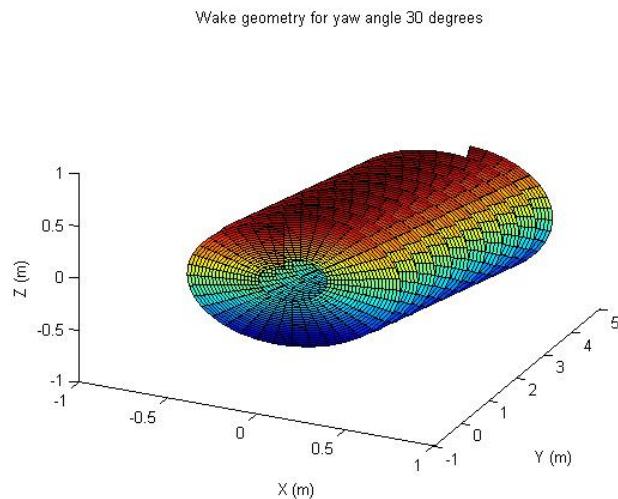


Fig. 11: Wake geometry for the case of a yaw misalignment

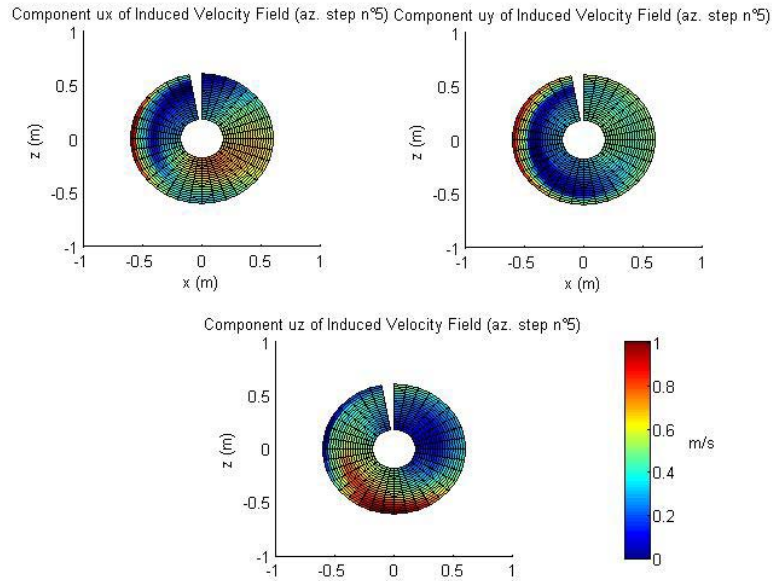


Fig. 12: *Induced velocities at rotor plane*

Conclusions

The great potential from active aerodynamic control on wind turbine blades for load reduction was thoroughly investigated in feedback control wind tunnel experiments. It was shown that fatigue loads on a dynamically scaled blade can be considerably reduced with such concepts. Regarding unsteady aerodynamic modelling, the prediction of unsteady aerodynamic response on 2d sections with controllable trailing edge flaps has been investigated and various cases show the potential in load reduction. 3d effects of the unsteady wake influence are also explored. Research in this field will be carried on at DUWIND, mostly focusing on full wind turbine aeroservoelastic modelling and scaled rotating experiments in the wind tunnel.

References

1. T. K. Barlas. Smart rotor blades and rotor control – State of the art – Knowledge base report for Upwind project W.P. 1B3, 2007.
2. T. K. Barlas and G. A. M van Kuik. State of the art and perspectives of smart rotor control for wind turbines. *In The Second Conference on the Science of Making Torque from Wind*, DTU, Denmark, 2006.
3. Troldborg N. Computational study of the Risø B1-18 airfoil with a hinged flap providing variable trailing edge geometry. *Wind Engineering*, 29, 2005.
5. Gaunaa M Buhl T and Bak C. Potential load reduction using airfoils with variable trailing edge geometry. *Solar Energy Engineering*, 127, 2005.
6. Gaunaa M Buhl T and Bak C. Load reduction potential using airfoils with variable trailing edge geometry. *In 43rd AIAA/ASME*, 2005.
7. Bak C Andersen P B, Gaunaa M and Buhl T. Load alleviation on wind turbine blades using variable airfoil geometry. *In 2006 European Wind Energy Conference and Exhibition*, 2006.
8. Bak C Andersen P B, Gaunaa M and Buhl T. Wind tunnel test on wind turbine airfoil with adaptive trailing edge geometry. *In 45th AIAA/ASME*, 2007.

9. Hulskamp A W, Beukers A, Bersee H, van Wingerden J W, and Barlas T K. Design of a wind tunnel scale model of an adaptive wind turbine blade for active aerodynamic load control experiments. In *16th ICCM*, 2007.
10. Theodorsen T. General theory of aerodynamic instability and the mechanism of flutter. *NACA Technical Report 497*, July 1935.
11. Bisplinghoff R. L., Ashley H., Halfman R L., *Aeroelasticity*, Addison-Wesley Publishing Co., 1955.
12. Leishman J G. Unsteady lift of a flapped airfoil by indicial concepts. *Journal of Aircraft*, 31, 1994.
13. Leishman J G. *Principles of helicopter aerodynamics*, 2nd edition, Cambridge aerospace series, 2006.
14. Sant T. Improving BEM-based aerodynamic models in wind turbine design codes, PhD Thesis, TUDelft, 2007.